Annual Review of Chemical and Biomolecular Engineering

Biological Assembly of Modular Protein Building Blocks as Sensing, Delivery, and Therapeutic Agents

Emily A. Berckman,[1,2,*] Emily J. Hartzell,[1,*] Alexander A. Mitkas,[1,*] Qing Sun,[3] and Wilfred Chen[1]

[1]Department of Chemical and Biomolecular Engineering, University of Delaware, Newark, Delaware 19716, USA; email: wilfred@udel.edu

[2]Department of Chemistry and Biochemistry, University of Delaware, Newark, Delaware 19716, USA

[3]Department of Chemical Engineering, Texas A&M University, College Station, Texas 77843, USA

Annu. Rev. Chem. Biomol. Eng. 2020. 11:35–62

First published as a Review in Advance on March 10, 2020

The *Annual Review of Chemical and Biomolecular Engineering* is online at chembioeng.annualreviews.org

https://doi.org/10.1146/annurev-chembioeng-101519-121526

*These authors contributed equally to this work.

Keywords

protein nanoparticles, biological assembly, posttranslational ligation, biosensing, drug delivery

Abstract

Nature has evolved a wide range of strategies to create self-assembled protein nanostructures with structurally defined architectures that serve a myriad of highly specialized biological functions. With the advent of biological tools for site-specific protein modifications and de novo protein design, a wide range of customized protein nanocarriers have been created using both natural and synthetic biological building blocks to mimic these native designs for targeted biomedical applications. In this review, different design frameworks and synthetic decoration strategies for achieving these functional protein nanostructures are summarized. Key attributes of these designer protein nanostructures, their unique functions, and their impact on biosensing and therapeutic applications are discussed.

INTRODUCTION

The development of effective therapeutic delivery vehicles and imaging reagents is of essential importance in medicine and healthcare. Over the past few decades, different synthetic carriers have been generated for these applications, fueled by advances in materials chemistry and nanotechnology (1). These systems provide sizable improvements in bioavailability, cellular uptake, and reduced side effects, but a significant technology gap exists in the ability of carriers to both efficiently capture and release nucleic acids and other complex biopharmaceuticals, which comprise a rapidly increasing portion of the pharmaceutical pipeline. Synthetic biology offers a powerful and streamlined platform for creating sophisticated, precisely organized nanostructures (2). Such approaches have key appeal in medicine because of their capacity to generate well-controlled architectures with inherent biospecificity. These architectures can provide critically needed improvements in biomedical applications, such as therapeutics and imaging, by enhancing the safety and efficacy of delivery vehicles.

Proteins must work together to perform a variety of complex tasks (3). In some instances, protein nanostructures are formed through specific molecular interactions of their fundamental building blocks to properly coordinate complex functions such as biosynthesis, cell structure, and cellular communication (4). Occasionally, additional functional and structural modules can be added through posttranslational modifications to expand the repertoire of functionalities (5). For example, viral capsids are perfect examples of a highly optimized natural protein complex that forms a stable polyhedral structure for protecting, storing, and transporting viral genetic information (6).

Synthetic biologists have taken inspiration from these native protein networks to develop modular protein assembly tool kits to create a broad spectrum of nanostructures (7, 8). These tool kits have now been exploited to generate many synthetic protein architectures for different applications, such as catalysis, sensing, and biomedicine (9, 10). One of the more important contributions in recent years is the design of smart protein nano-assemblies for selectively targeting tissues for sensing and therapeutic applications (11). The use of well-defined nanostructures is highly relevant for biomedical applications given the stringent demands for stability, biocompatibility, and biosafety. The ability to combine multiple functionalities into a single protein nanostructure can help guide the desired localization and the preferred distribution of therapeutic agents to the disease site rather than healthy tissues (12).

Although rapid progress in chemical modifications has been made in the last decade, this strategy is still considered less attractive for the assembly of protein building blocks owing to lack of control of site selectivity and orientation, resulting in reduced bioactivity (13). In contrast, biological assembly tools have met with some notable success in engineering entirely new protein nanostructures (14, 15). Many well-known and de novo design noncovalent protein–protein interaction pairs, such as coiled-coil domains, have been used to induce protein assembly to form distinct 3D nanostructures (16). In parallel, new bioconjugation strategies are now available to provide controlled modifications of both the exterior and interior of protein nanostructures in benign conditions (17). The ability to allow dynamic assembly has begun to emerge as a new way to provide spatial and temporal control of material properties for improved efficacy (18). In this review, we focus on the use of biological approaches to assemble modular protein building blocks into functional nanostructures as sensing, targeting, and therapeutics agents (**Figure 1**). We first discuss the various scaffolds and tool kits available to provide multifunctionalization before highlighting their prospective use in the field of biomedicine.

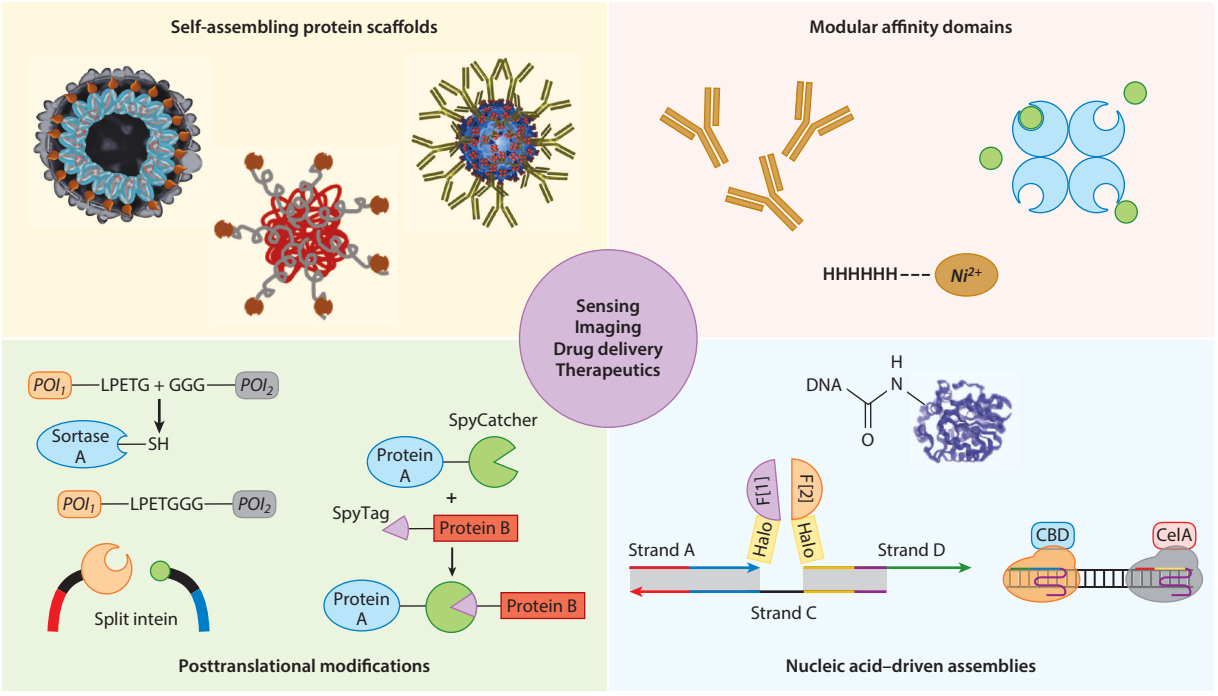

Figure 1

We focus on the use of biological approaches to assemble modular protein building blocks into ordered and functional nanostructures as sensing, targeting, and therapeutics agents. Many of these nanostructures are derived from self-assembling proteins, such as virus-like particles, ferritin, and non-native synthetic cages. A wide variety of self-assembling affinity domains and posttranslational conjugation strategies are used to decorate these nanostructures with customized functionalities. Dynamic modulation of functionalities can also be executed using nucleic acid–based assembling strategies.

SELF-ASSEMBLING PROTEIN SCAFFOLDS

Virus-Like Particles

Self-assembling protein nanoparticles have gained attention as a promising scaffold for biomedical applications because of a wide range of available sizes. Specifically, viral nanoparticles as well as virus-like particles (VLPs), which lack the genome of natural viruses, have been used in a plethora of medical applications from drug delivery devices to diagnostic reagents and even vaccines (12). The viral capsids are typically made up of hundreds of subunits that self-assemble into a protein nanocage. These cage-like assemblies come in a multitude of sizes and various morphologies, such as filaments, spheres, and icosahedral structures (19). Extensive research has been focused on the use of VLPs, as they lack the endogenous genetic material, allowing for an empty interior perfect for a large variety of cargos (20). The interior of VLPs can then be modified to be more accommodating to different cargos of interest (21). Owing to the wide variety of VLPs, the cargo possibilities span from polymers and drugs to fluorescent proteins and magnetic resonance (MR) contrast agents (22). The exterior of VLPs can be modified with a variety of proteins, such as antigens for vaccines, peptide ligands for targeting, and peptide tags for purification and detection (8). The multi-valency of these exterior decorations makes VLPs an ideal candidate for a multitude of applications.

Table 1 List of virus-like particles discussed

Protein cage	Species	Shape	Size (nm)	Applications
P22	*Salmonella typhimurium*	Icosahedral	58–64	Biocatalysis
Qβ	*Escherichia coli*	Icosahedral	28	Biosensor Delivery
CCMV	Cowpea plant	Icosahedral	28	Biocatalysis
HBV	Human	Icosahedral	30–34	Biosensor Vaccine Delivery Magnetic resonance imaging
MS2	*E. coli*	Icosahedral	27	Biosensor
M13	*E. coli*	Filamentous	7 × 880	Biosensor
E2	*Bacillus stearothermophilus*	Spherical	24	Biocatalysis Biosensor Delivery
Small heat shock proteins	*Methanococcus jannaschii*	Spherical	15–20	Cancer Therapy
Ferritin	*Human*	Spherical	12	Delivery Magnetic resonance imaging
Ferritin	*E. coli*	Spherical	12	Photothermal therapy
Ferritin	*Pyrococcus furiosus*	Spherical	12	Biosensor Magnetic resonance imaging
O3–33	Synthetic	Octahedral	13	TBD
T3–10	Synthetic	Tetrahedral	11	TBD

VLPs from different species are known to offer unique qualities that can be used for different applications (**Table 1**). For instance, the bacteriophage Qβ forms icosahedral capsids from 180 coat proteins (CPs) that encapsulate its RNA genome by virtue of the high-affinity interaction between a hairpin structure on the RNA and interior-facing residues of the CP (23). This particular VLP has four disulfide bridges that help stabilize the capsid at temperatures up to 75°C, making it one of the stablest VLPs for in vivo applications. The disulfide bonds also allow the stability of the capsid to be modulated by the redox potential (24). Another interesting bacteriophage P22 can self-assemble into a 58-nm capsid based on the interaction between the CPs and a helix-turn motif on the scaffolding proteins (17). The unique scaffolding protein can specifically direct guest proteins of interest into the VLP with high loading efficiency and can be used to simultaneously encapsulate multiple functional proteins to the interior (25). The bacteriophage M13 offers a different rod-shaped VLP structure and contains a few copies of the P3 CP at the tip and more than 3,000 P8 CPs on the entire surface (26). The ability to add functionalities to either the tip or the surface of M13 in an orthogonal manner offers unique opportunities to enhance cellular targeting and detection sensitivity.

In addition to bacteriophages, human and plant viruses are also of great interest, as they are usually larger and provide a larger surface for modifications. Hepatitis B virus (HBV)-based capsids offer a flexible nanocarrier system, as they can be expressed in *Escherichia coli* in high yields and their structures can tolerate insertions of foreign proteins to the interior as well as the exterior (27). Physical linkage between N- and C-cores of HBV is not necessary for capsid assembly, and functional capsids can be assembled using fragment complementation of the separately expressed N- and C-cores (SplitCore) (28). Expressing the N-core and C-core fragments as separate proteins gives two exposed termini on the surface of the capsid that can be easily decorated with

protein partners. Cowpea chlorotic mottle virus (CCMV) from the plant Bromoviridae family is another interesting VLP that undergoes a reversible pH-dependent swelling (12). CCMV VLPs can reversibly assemble in a pH-dependent manner and allow easy encapsulation of cargos based on electrostatic interactions with the interior (29). The capsids fall apart into dimers when the pH is increased to 7.5 and reassemble upon lowering back to pH 5.0. The reversible assembly of CCMV capsids has been used to encapsulate different types of cargoes, such as MR imaging contrast agents and enzymes (29). This pH-dependent control allows the CCMV to trigger the release of entrapped cargos.

Nonviral Protein Nanocages

Aside from self-assembling cages derived from viruses, nature has also designed other proteins that self-assemble into ordered structures of various sizes and shapes (30). Their nonviral origin alleviates potential safety concerns associated with using pathogen-derived materials in in vivo applications. Although these nanocages are from different origins than VLPs, they share several key attributes: the ability to decorate the exterior of the cage; internal encapsulation of cargos; and applications in sensing, delivery, and therapeutics (**Table 1**).

Ferritin is responsible for iron homeostasis, using its core for iron detoxification and iron reserves. Structurally, ferritin is composed of 24 protein subunits, resulting in a 12-nm hollow spherical cage with an interior space 8 nm in diameter (31). One key feature of ferritin is its extreme stability in non-native conditions (high pH values nearing 9 and temperatures up to 85°C). Whereas ferritin nanocages are stable at high pH values, they disassemble at pH 2–3. This pH responsiveness can be used for encapsulating selected cargos that are not pH liable (32).

Small heat shock proteins (sHsps) are expressed in response to elevated temperatures. They are chaperones responsible for aiding proteins in forming their correct folding structures (32, 33). sHsps are endogenous to many species, though considerable work in terms of nanocages has been focused on those from the hyperthermophilic archaeon, *Methanococcus jannaschii*. This particular sHsp nanocage self-assembles into a spherical structure with an internal cavity 6.5 nm in diameter and a large pore size of 3 nm, which allows for small molecules to freely diffuse in and out (34). sHsps can also be decorated with exterior peptides. For example, the exterior of the sHsp was modified to express the RGD peptide, which is capable of targeting integrins upregulated in many cancers (35).

The E2 nanocage derived from the pyruvate dehydrogenase complex from the thermophilic bacterium *Bacillus stearothermophilus* is another attractive protein nanocage because of its intrinsic stability under extreme conditions (7). More importantly, the surface exposure of the N terminus makes it feasible to add functionalities to the surface of E2 for cell targeting; however, these are limited to small peptides (36).

Synthetic Protein Nanocages

An emerging alternative to naturally occurring nanocages is to artificially engineer protein-based nanoparticles (37). Efforts have been made in engineering matching protein symmetries to drive their linear, planar, and tetrahedral self-assemblies (38–40). However, most of these studies rely on expensive computational design, and the available building blocks are still limited to achieve the required atomic-level accuracy. The first successful rational approach to create highly ordered self-assembled protein nanostructures is based on the use of a dimeric and a trimeric protein domain that are held together in a predetermined orientation by genetic fusion (**Figure 2*a***).

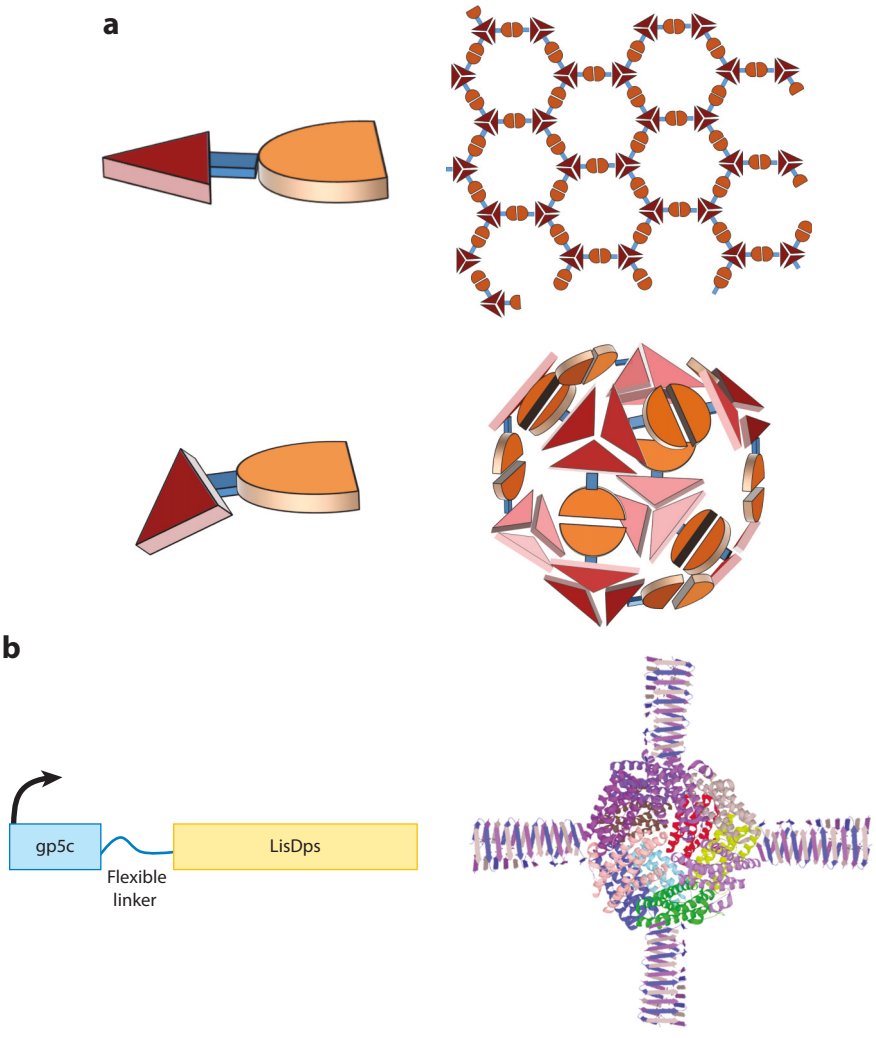

Figure 2

Self-assembled protein nanostructures based on two multimeric proteins. (*a*) A fusion between a dimeric and a trimetric protein is used to assemble into either a 1D or a cage-like nanostructure. The interface geometry plays an important role in controlling the formation of different nanostructures. (*b*) The same platform has been used to form ball-and-spike nanoparticles.

The precise orientation between the two domains is controlled by adjusting the rigidity of the linker peptide to achieve the desired tetrahedral cage-like structures (38). Replacing the trimeric building block with a second dimeric partner results in the formation of protein filaments via head-to-head and tail-to-tail interactions. This simple design rule has been adopted to create other predefined ball-and-spike (41), lattice, and cage-like nanostructures (**Figure 2*b***) (42). To increase the versatility of building blocks beyond fusion proteins, several noncovalent methods, such as coiled-coil (16) interactions, have been used to link the oligomeric domains into desired nanostructures (43). A trimeric esterase (TriEst) was fused to a well-characterized pentameric parallel coiled-coil domain to generate 60-subunit icosahedral protein nanocages that are highly

stable (44). These examples highlight the structural flexibility achieved simply by creating the appropriate pairwise interactions.

Synthetic protein nanocages with defined structures have also been computationally designed by defining the required protein–protein interfaces for self-assembly (45) (**Table 1**). This strategy has been used to create synthetic viral-like icosahedral structures using a wide range of two-component building blocks (46). One unique property of using two distinct multimeric protein components is the possibility of in vitro self-assembly through simple mixing of the different components. Although computational models can design a library of possible structures, extensive experimental evaluation is still necessary to select the few designs that actually form stable structures.

Other Synthetic Protein Nanostructures

Elastin-like polypeptides (ELPs) are composed of the repeating pentapeptide subunit (VPGXG) (X: any amino acid except P) (47). ELPs exhibit reversible self-assembly or coacervation behavior in response to changes in temperature and salt concentration (47). Because their transition properties can be precisely controlled at the genetic level by modulating molecular weight and composition, ELPs can be expressed as block copolymers to drive their self-assembly into nanoparticles ranging from 20 to 40 nm in diameter (48). Specific ligands can be presented onto the corona of the spherical micelles for a wide range of applications (49).

Other self-assembled peptide pairs, such as coiled-coil domains and leucine zippers, have also been exploited for nanostructures for applications in sensing, drug delivery, and therapeutics. In its most basic form, a coiled-coil is a bundle of α-helices that are wound together, driven by hydrophobic and charged amino acids, forming a superhelix with a hydrophobic core and interhelical salt bridges (50). Many scientists have used various engineering techniques to form more predictable and stable coiled-coils of various sizes and shapes (50). In one example, a de novo hexameric coiled-coil bundle was used to generate a protein nanocarrier roughly 10 nm in diameter (51). A wide range of other coiled-coil domains with well-defined multimeric structures have also been used to generate other nanostructures, including nanotriangles (52). Similarly, ELP–leucine zipper fusions have been used to recruit the corresponding zipper–green fluorescent protein (GFP) fusion to self-assemble into micron-sized micelles (53). The flexibility in recruiting a wide range of target proteins into the micelle structures makes this an ideal strategy for generating micelles with multiple functionalities.

Recently, a newly discovered protein, suckerin, was found to form supramolecular structures, stabilized by nanoconfined β-sheets. Synthetic biologists have engineered these native proteins to form artificial suckerin-19 (S-19) proteins that can function as nanocarriers for various applications (54). Ping et al. (55) have harnessed the benefits of the S-19 proteins to form self-assembling nanoparticles of varying sizes (100–200 nm) that can be used to encapsulate hydrophobic drugs as well as DNA.

DECORATION OF PROTEIN NANOSTRUCTURES

Direct genetic fusion is perhaps the easiest strategy to decorate protein nanostructures with additional functionalities. In some cases, peptides can be directly inserted into either a surface-exposed N or C terminus or an exposed surface loop of VLPs without any impact on the overall folding (56). Selected peptides can also be tethered to the interior of nanocages via direct genetic fusion (17, 57). Although some small proteins can also be genetically tethered using the same strategies, their success has been limited, as they have a higher tendency to disrupt the nanocage structure

(58). More importantly, functional moieties such as chemical dyes, drugs, inorganic nanoparticles, and nucleic acids cannot be added in this manner. Although many chemical conjugation methods are available, they tend to deactivate the target proteins and also lack the ability to properly orient the functional motifs (59). For these reasons, we instead focus our discussion on the use of self-assembling affinity domains and posttranslational conjugation strategies for decorating these nanostructures with multiple functionalities.

Modular Affinity Domains for Protein Assembly

In nature, protein–protein interactions are commonly used to cluster different biological components together for targeted outputs (60). These interactions are highly specific and have been exploited as synthetic building blocks to enable the formation of structurally defined protein complexes. We highlight some of the more relevant interaction pairs for biosensing and drug delivery and discuss how they can be used to provide functional decoration.

Antibody Binding Domains

The high binding and specificity of antibodies have made them attractive in therapeutic targeting, as well as in the development of highly sensitive sensing and imaging tools. The proper assembly of antibodies into therapeutic and diagnostic devices is crucial in maintaining their specificity and sensitivity (61). Physical adsorption and chemical conjugation have been used for both solid-phase assays and antibody-linked therapeutics. The weak, nonspecific, and hydrophobic interactions in adsorption, however, are not stable over repeated washings (62), and chemical conjugation targeting lysine residues can alter the binding region (62). Additionally, these methods provide no control over antibody orientation, which has been shown to impact sensitivity (61–63). An ideal assembly strategy is to specifically target the Fc domain to allow the antigen binding (Fab) domain full access to its respective antigen or therapeutic target. Modular antibody binding domains (ABDs) have gained attention in serving as adaptor units that site-specifically dock and orient antibodies onto sensing and therapeutic devices. Such modular adaptor components bind a variety of antibody types from different sources (63–65) and can therefore be used in a plug-and-play manner, allowing the respective device to be repurposed toward virtually any target (66, 67).

Protein A from *Staphylococcus aureus* and streptococcal protein G are the most widely used ABDs, as they bind mainly to the Fc domain of a wide variety of antibody species (64, 65, 68). Protein A contains five homologous, tri-helical domains (E, D, A, B, C) that are 58 amino acids in length (69), each of which can separately bind the Fc of IgG. Domain D, however, has also been shown to bind to the Fab portion (70). Domain B is the most common minimal binding domain used and binds only the Fc domain of the antibody. Domain B has been further engineered into the Z-domain, which is a more chemically resistant derivative (69). Z-domains can be used individually to bind antibodies but can also be displayed in tandem repeats to increase avidity and apparent binding affinity (71). Although protein G binds to the same region of the Fc domain, it shares no homology with protein A (72). Protein G contains three homologous C-terminal IgG-binding domains (C1, C2, and C3), each of which are 55 amino acids in length (65). The C2 domain binds only the Fc portion of the antibody, whereas the C1 and C3 domains bind both the Fc and Fab (72, 73); however, mutagenesis can be performed to abolish Fab binding (62). Proteins A and G are highly soluble fusion partners and are used in orienting antibodies on solid-phase surfaces for sensing applications (66, 74). They are also displayed on protein nanoscaffolds for the modular recruitment of antibodies (10, 26, 61).

Although proteins A and G and their derivatives have been used in a variety of applications, their size and instability are not ideal for repeated use or long-term storage. Additionally, there are immunogenic concerns with using bacterially derived proteins for in vivo applications. A diverse set of Fc-binding peptides containing linear, branched, and cyclic structures have been discovered through phage display for antibody purification (75). In particular, the high-affinity, cyclic Fc-III peptide, which was found to bind the same region of the Fc as proteins A and G (76), strongly bound human IgGs 1 and 2, as well as rabbit IgG, and moderately bound mouse IgG3 (63). The peptide-conjugated surface was stable through repeated NaOH washes, and bound antibodies performed 1.6 times more efficiently than randomly conjugated antibodies. Fc-III was fused into the loop of a ferritin cage, where the fourfold symmetry provided avidity, increasing the apparent affinity of the peptide (77).

The noncovalent nature of ABDs limits their use in multiplexing in imaging and many in vivo applications. The site specificity to the Fc domain, however, can be used to direct covalent bond formation between an antibody and desired conjugate. Either photoactivable benzophenone groups are coupled to cysteines mutated within the ABD (62, 78, 79) or benzoylphenylalanine is incorporated as an unnatural amino acid (80–82). Upon UV irradiation of an ABD antibody complex, a covalent bond is formed with approximately 50–80% conjugation efficiency, depending on the location of the photoactive group, type of ABD, and method of photoactive group incorporation. These covalent complexes are used for stable coupling to solid-state sensor chips (62), site-specific labeling with fluorescent dyes (81) or superparamagnetic iron oxide nanoparticles (80), protein fragment complementation assays (78), and pretargeting for radionuclide molecular imaging (79).

Biotin–Streptavidin

The femtomolar affinity of the biotin–streptavidin pair has made it popular for use in the noncovalent assembly of proteins in sensors and therapeutics. Thus, many biotin- and streptavidin-coupled antibodies, detection agents, and surfaces are commercially available for these applications. Biotinylation of recombinant proteins is typically preferred over direct fusions to streptavidin, as streptavidin is often expressed in inclusion bodies in *E. coli* (83). N-hydroxysuccinimide ester chemistries are traditionally used for the biotinylation of lysines; however, the nonspecific nature of the chemistry can decrease the activity of the biotinylated protein (62, 84). In nature, biotin holoenzyme synthetases catalyze site-specific biotinylation to biotin carboxyl carrier proteins, where the sequence around the biotinylated lysine is conserved across many species (85). A minimal 14–amino acid peptide (GLNDIFEAQKIEWH) was discovered that could be site-specifically biotinylated with high efficiency by *E. coli* biotin holoenzyme synthetase BirA. Recombinant protein fusions to the biotin acceptor peptide (BAP) can be biotinylated either in vitro or in vivo in both bacterial (84) and mammalian (86) hosts by co-expressing the BirA.

The BAP is especially valuable in assembling antibody fragments such as single-chain variable fragments (scFv), antigen-binding fragments (Fab), and nanobodies, as they lack the Fc domain and cannot be oriented with an ABD. Immobilization through site-specifically biotinylated antibody fragments provides more sensitive detection than immobilization through adsorption (87) or chemical biotinylation (84). The BAP can also be incorporated into nanoparticle structures, including amyloid fibers (88) and icosahedral VLPs (89), through fusion to monomeric components for the modular incorporation of detection moieties or cargo. Additionally, the tetravalency of the streptavidin protein allows crosslinkage of multiple biotinylated moieties. A BAP-fused scFv that targets prostate stem cell antigen was used for pretargeting for radio immunotherapy (90). The scFv provides high penetration of the tumor environment and a long residence time at the tumor

site. It is linked to one of the NeutrAvidin binding sites, so that the smaller radio-labeled biotin can bind at the tumor site and rapidly clear from the rest of the body, lowering systemic toxicity. The tetravalency of streptavidin has also been used to create multivalent antibody structures, such as bispecific antibodies and tetravalent Fabs for in vivo imaging (86).

His-tag Coordination with Nickel

The micromolar interactions between histidine-rich domains and transition metals have been well studied in the development of immobilized metal affinity chromatography (91). The imidazole groups on the histidines coordinate with the open valencies of metal ions supported on chelating ligands. The most popular of these is Ni^{2+} and nitrilotriacetic acid (Ni-NTA), in which the NTA coordinates with four valencies on the Ni^{2+} ion, leaving space for the coordination of two histidine residues. The oligo histidine tag (92), or His-tag, containing 6–10 adjacent histidines, is the most commonly used. It has also been applied for the oriented immobilization of proteins onto Ni-NTA-coated solid surfaces for enzyme-linked immunosorbent assays and surface plasmon resonance sensor applications (74). The advantages of using these domains are that the protein binding is reversible and the Ni-NTA can easily be recycled for multiple uses by displacing the His-tagged protein with high concentrations of imidazole or chelating out the nickel with ethylenediaminetetraacetic acid. Adding a small His-tag fusion to an ABD can orient the molecule to maximize active binding spots for antibody capture, providing higher sensitivity than physically adsorbed antibodies (74).

His-tag/Ni-NTA interactions can also be used to immobilize proteins and inorganic materials on protein nanoparticles. A modular imaging tool was created by fusing human heavy-chain apoferritin monomers to a His-tag, where the His-tag can recruit Ni-NTA-coated detection components, such as quantum dots, gold nanoparticles, and magnetic nanoparticles, for a variety of imaging applications (67). Ni-NTA has also been conjugated to potato virus X to display His-tagged tumor necrosis factor–related apoptosis-inducing ligand (TRAIL) (93). In this application, TRAIL orientation is important for promoting apoptosis in cancer cells. The TRAIL presented on the nanoplatform had 3–10-fold-lower IC_{50} compared with soluble TRAIL in different triple-negative breast cancer cell lines and outperformed soluble TRAIL in inhibiting tumor growth in athymic nude mouse models. Because the Ni-NTA interaction is weak and there are concerns over the stability and toxicity of the domains for in vivo applications, loading the interior cavities of protein nanoparticles may be a better use for this technology. Ribonucleoprotein vaults have been loaded with Ni-NTA-coated gold nanoparticles by fusing a His-tag to the minimal interaction domain that binds the interior of the vault (94). The gold nanoparticle was also used to crosslink additional His-tagged GFP for loading into the vault. Ni-NTA has also been conjugated to the N terminus of solid-phase synthesized β-annulus peptide 1, derived from the tomato bushy stunt virus, which self-assembles into dodecahedral virus-like nanocapsules (95). Particles were assembled with His-tagged GFP and encapsulated the GFP with 91% efficiency.

Posttranslational Conjugations for Protein Assembly

Protein assembly through posttranslational modification is a powerful approach for creating specifically tailored protein–protein or protein–small molecule hybrids. Posttranslational ligation offers an orientation-specific, robust approach to developing potent sensing, delivery, and therapeutic platforms. The most successful approaches recently employed Sortase A (SrtA)-catalyzed reactions, intein chemistries, and SpyTag/SpyCatcher isopeptide reactions to generate novel protein assemblies. All these ligation techniques are characterized by efficiency and selectivity and can

Table 2 Comparison between the three different approaches for posttranslational modifications of proteins

Technique	Kinetics	Reversible	Orthogonality	Scar size	Downstream purification	Small-molecule conjugation
Sortase A	Fast	Yes	Yes	5 amino acids	Yes	Yes
Intein	Slow	No	Yes	Scarless	Yes	Yes
SpyCatcher/Tag	Fast	No	Yes	123 amino acids	No	No

be carried out in vitro, allowing for one-pot reactions for multiple modifications through simple mix and match (**Table 2**).

Sortase A

SrtA from *S. aureus* is a powerful enzyme for site-specific protein, peptide, and small-molecule incorporation (**Figure 3*a***). It catalyzes a peptide bond formation between a C-terminal R_1–LPXTG motif and an N-terminal $(G)_n$-R_2 motif. The active site of SrtA cleaves the –LPXTGXX motif between the threonine and the glycine, which can then be attacked by the oligoglycine-tagged moiety to form a new peptide bond, resulting in the formation of a R_1–LPXTGGG-R_2 construct (14). Because the end product also contains a –LPXTGXX motif, it can in turn be reacted upon by SrtA. Typically, to avoid reversing the reaction, one of the two reactants is added in excess or by physically removing the glycine peptide fragments generated from the initial cleavage (96).

Improving the yield and reaction rates of SrtA-catalyzed reactions and discovering alternative recognition motifs have helped the technology become more versatile. One of the most common variants of SrtA has either the first 25 or 59 residues removed (96). Although this variant is functional, the Ca^{2+} requirement and low reaction rates can be problematic. Directed evolution has successfully yielded a mutant that resulted in a ~120-fold increase in the k_{cat}/K_M relative to the native protein. Two further mutations removed the Ca^{2+} dependency while retaining the improved activity (96). Furthermore, SrtA variants with different recognition motifs have been discovered to provide orthogonal modifications to proteins. SrtA isolated from *Streptococcus pyogenes* recognizes the LPXTA motif and has been used in conjunction with the *S. aureus* version for orthogonal labeling of the M13 capsid proteins (97, 98). The improved and orthogonal versions of SrtA can help expand the industrial applications and commercial production of biotherapeutics.

Overall, SrtA allows the ligation of proteins to other proteins, peptides, and small chemical compounds with minimal scarring (LPXTG/A). Owing to the nature of the ligation, the final products have specific orientation, allowing the production of homogeneous therapeutic compounds. The reaction itself is rapid and requires minimal optimization. However, subsequent purification of the product is required to eliminate the SrtA and unreacted substrates. The reaction also allows only N/C-terminal fusions, limiting the valency of the final product. Intein-mediated posttranslational ligation is an alternative method that minimizes the need for downstream purification, offers potential scarless ligation, and has minimal primary sequence constraints.

Inteins

Inteins are self-excising peptide sequences discovered in eukaryotic organisms that are analogous to RNA introns. Inteins can be expressed as a whole piece, which is self-catalytically excised while simultaneously linking the flanking N and C exteins (99) (**Figure 3*b*,*i***). Split inteins can be created in which an N-intein and a C-intein are used to join, excise, and ligate two target protein pieces together (**Figure 3*b*,*ii***). For intein excisions to occur, the C terminus of the extein must

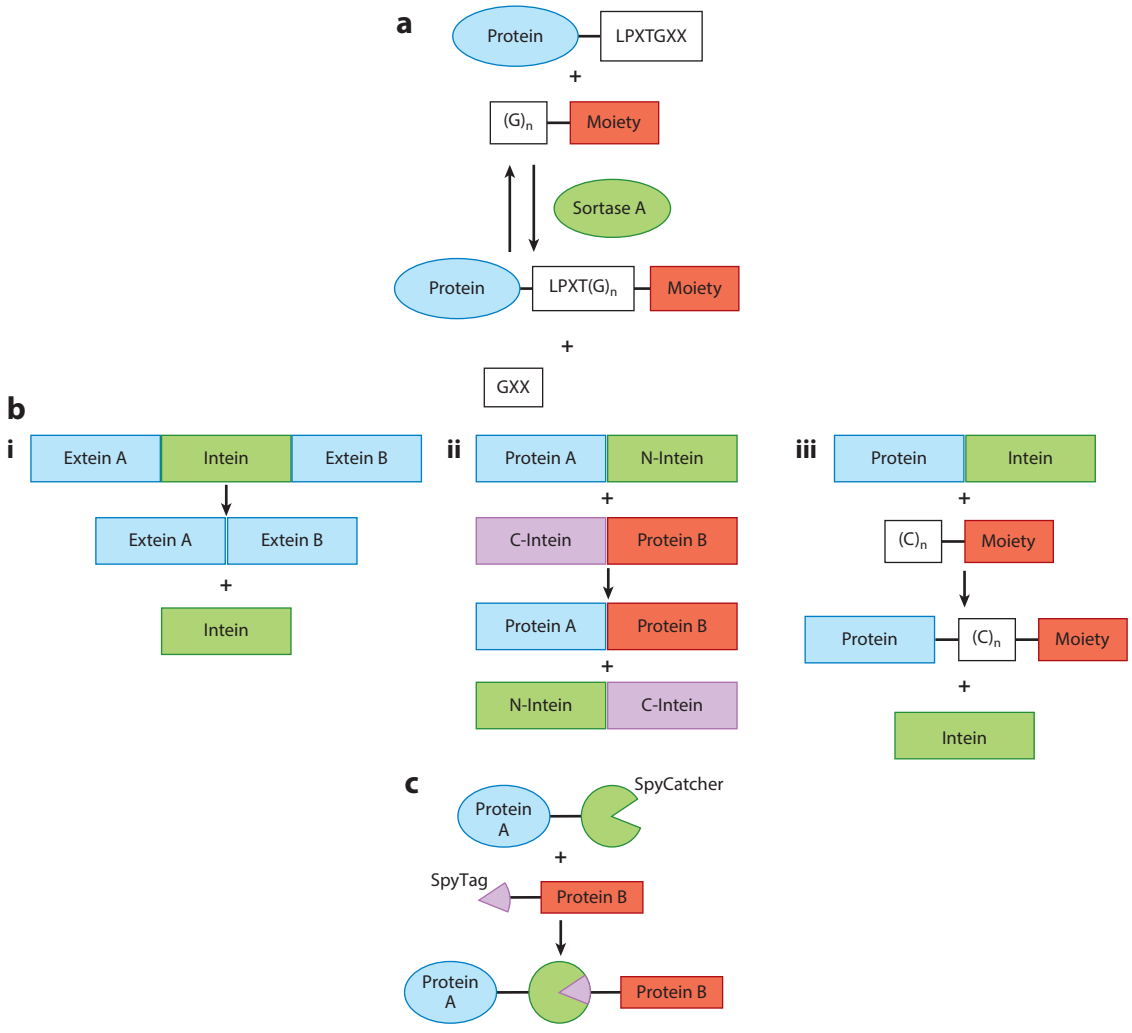

Figure 3

Summary of bioconjugation strategies. (*a*) The mechanistic action of Sortase A–catalyzed transpeptidation. Sortase A cleaves between the Thr and Gly residues in the LPXTG motif and catalyzes the formation of a peptide bond between the carboxyl group of threonine and the amine group of the Gly attached to the moiety. (*b*) Three different modes of intein-mediated ligation. (*i*) Native intein excision. The process is characterized by a series of acyl-transfer reactions that result in the breaking of two peptide bonds at the intein–extein interface and the formation of a new peptide bond between the two exteins. (*ii*) Split inteins are transcribed as two distinct polypeptides. The N and C terminus split inteins spontaneously and noncovalently associate with each other upon mixing. The resulting intermediate closely resembles the structure of a full-length intein and self-excises itself from the remaining peptide sequence through the same mechanism full-length inteins use. (*iii*) Addition of a small chemical moiety via thioester chemistry and intein cleavage. Proteins with a Cys residue followed by an intein that can excise itself through standard intein chemistry and in the process generate α-thioester groups at the C terminus of the protein next to the cystein. The α-thioester group can be reacted with 1,2-aminothiol, cysteinyl, or other nucleophilic groups conjugated to small-molecule chemicals to form a covalent bond between the protein and the small molecule with minimal scarring (1 Cys residue). (*c*) Spontaneous conjugation between SpyTag and SpyCatcher via the formation of an isopeptide bond between the Lys in the SpyCatcher and the Asp in the SpyTag.

be a cysteine, serine, or threonine reside. Split inteins used in conjunction with an extein that has a C-terminal cysteine can be used to generate α-thioester moieties on the proteins, which can be reacted with 1,2-aminothiol groups or other nucleophiles to conjugate small molecules and peptides to proteins (100) (**Figure 3*b*,*iii***). Split-intein ligation can be engineered to be scarless, leaving no extra amino acids in the primary sequence of the ligated proteins or peptides (101).

Inteins can be categorized as full-length and mini inteins based on their size. Full-length inteins contain a homing endonuclease domain (HED) that allows for insertion of the intein DNA sequence in other areas of the genome at recognized motifs. Mini inteins lack the HED and are considerably smaller in size (~100 amino acids) (99). Intein splicing does not require the HED; thus, mini inteins are more suitable for most engineering applications (100). Side reactions that involve only N- or C-terminal cleavage can yield unwanted products but can also be harnessed for applications such as tagless purification by controlling the reaction conditions. C-terminal cleavage of inteins is pH dependent, thus allowing for controlled release of the intein through pH control of the reaction (99). Although the intein family of proteins is vast, most engineering applications rely on the use of split inteins for the conjugation of different proteins or proteins to small chemical molecules.

Inteins provide a powerful platform for scarless posttranslational assembly of components for development of sensing, delivery, and therapeutic platforms. Split-intein strategies are simple and require only the addition of a Cys residue for ligation. However, intein reactions can be slow, taking up to 24 h to proceed to completion, and are plagued by low reaction yields. Furthermore, intein fusions are notoriously insoluble in microbial systems, making it difficult to execute in vivo ligation in some cases (102). The SpyTag/SpyCatcher system is an alternative posttranslational modification technology that offers fast and efficient conjugation via an isopeptide bond formation.

SpyTag/SpyCatcher

The SpyTag/SpyCatcher system involves the spontaneous formation of an isopeptide bond between the 13-residue SpyTag and the 116-residue SpyCatcher (**Figure 3*c***). The system is derived from the CnaB2 domain of the fibronectin-binding protein FbaB from *S. pyogenes* (103). The SpyTag and SpyCatcher pair can rapidly form an isopeptide bond under both in vivo and in vitro conditions. The SpyTag/SpyCatcher system offers a versatile system to encode posttranslational protein assembly in biologically relevant environments. The nature of the isopeptide bond formed means that the assembly can occur at most positions in the protein sequence and not only at the N and C termini. Progress toward shortening the tags has also resulted in the SpyLigase system, in which the SpyCatcher active domain (KTag) is the only sequence that needs to be added. The ligation between the SpyTag and the KTag is then catalyzed by SpyLigase, which requires separate expression and is composed of the remainder of the SpyCatcher residues (104). Unfortunately, the SpyLigase system lacks the efficiency of the SpyCatcher/SpyTag system, which limits its applications.

Inspired by the SpyTag/SpyCatcher system, other protein pairs capable of spontaneously forming isopeptide bonds have been created. Specifically, the SnoopTag/SnoopCatcher isolated from *Streptococcus pneumoniae* (105) and the SdyTag/SdyCatcher isolated from *Streptococcus dysgalactiae* (106) represent two additional pairs also able to form isopeptide bonds. The availability of orthogonal Tag/Catcher systems opens up new avenues of more complex modifications. Orthogonal reactions using Spy and Snoop pairs have been successfully employed for twin antigen immunization (107). Use of the Sdy pair also could allow for the potential of up to three desired proteins

to be ligated on the same target protein. Furthermore, decorating nanoparticles with distinct tags could allow the simultaneous decoration of the nanoparticle with different functional groups in a manner that can control the ratio and absolute level of the functional groups. In engineering systems for sensing, delivery, and therapeutic applications, the presence of orthogonal tools with similar efficiency allows the creation of tailor-made solutions to distinct problems.

Although the orthogonal Tag/Catcher pairs allow for more complex architectures by allowing the addition of different moieties at specific locations and ratios, the scarring left behind is significantly larger. Furthermore, SpyTag/SpyCatcher is preferable only when conjugating proteins to other proteins or peptides. When adding small chemical moieties to the desired protein, SrtA or intein ligation is preferable owing to the smaller requirement of amino acid additions. Overall, if the area in which the SpyTag/SpyCatcher domain is inserted does not impact the function of the protein, and the ligated components are both peptide based, it is a powerful tool for posttranslational protein assembly in vivo and in vitro.

In summary, all three posttranslational modification techniques discussed can create exciting and smart solutions to sensing, delivery, and therapeutic problems. Although there is overlap between the applications of the technologies, they each come with their own advantages and disadvantages. Combining these posttranslational assembly strategies to generate dynamic components with on-cue assembly/disassembly can be a powerful tool for creating smart delivery, sensory, and therapeutic products.

BIOSENSING AND THERAPEUTIC APPLICATIONS

Proteins provide a diverse selection of functional properties relevant to bioassays, bioimaging, and drug delivery. A device for such applications consists of an input domain, an output domain, and an adapter between the two. Input components can be sensing or cell-specific targeting domains, such as antibodies, antibody fragments, and other affinity binders. Output components include detection agents, such as colorimetric enzymes and fluorescent or luminescent reporters, and therapeutic agents, such as chemotherapeutics, siRNA, and protein toxins. Their assembly onto a protein or nucleic acid nanoscaffold adaptor provides desirable properties, such as signal amplification for sensing and imaging, increased avidity for antigen capture and cell targeting, and an increased therapeutic payload. Examples of how the previously detailed scaffolds and assembly strategies are used in these practical applications are presented below.

Bioassays

To create highly sensitive assays, high packing density of the sensing domains in controlled orientation is critical. Small His-tag insertions provide a simple means of controlling the orientation of proteins on nickel surfaces. His-tagged protein A pods, which could pack five capture IgGs per pod, were immobilized onto nickel surfaces, which provided a 64-fold higher sensitivity than physically adsorbed antibodies in an ELISA setting (74). The higher-affinity binding of biotin–streptavidin can be used for further sensitivity, and controlled orientation can be achieved through fusions to the BAP. An scFv-BAP fusion targeting glycocholic acid was employed in an ELISA and provided higher sensitivity compared with randomly biotinylated scFv (84). Similarly, a sandwich ELISA using BAP-fused nanobodies for the detection of influenza virus had a lower limit of detection (14.1 ng/mL) than surface-adsorbed nanobody (500 ng/mL) (87). Intein chemistry can also be used for site-specific biotinylation (108). A matrix metalloprotease sensor was made through a luciferase fusion to a substrate peptide and intein, where uncleaved, biotinylated protein was captured by NeutrAvidin-coated plates. Although SrtA can biotinylate proteins as well,

stabler immobilization can be achieved by directly ligating the protein to the surface (109). Similarly, the SpyTag/SpyCatcher system was used to covalently immobilize single-domain antibodies in specific orientation on solid support, which increased the detection limit for the dengue virus nonstructural protein 1 by fivefold (110).

Capture density of sensing domains can be further enhanced by expanding the binding surface onto 3D scaffolds (30, 61). These protein nanoparticles, named proteinticles, are made from multiple monomer subunits fused to one or two tandem B domains from protein A, which self-assemble into uniform structures displaying the ABDs at high density (30) (**Figure 4*a***). The symmetry of the assembled proteinticles additionally provides hot spots of B domain with lower K_D at the

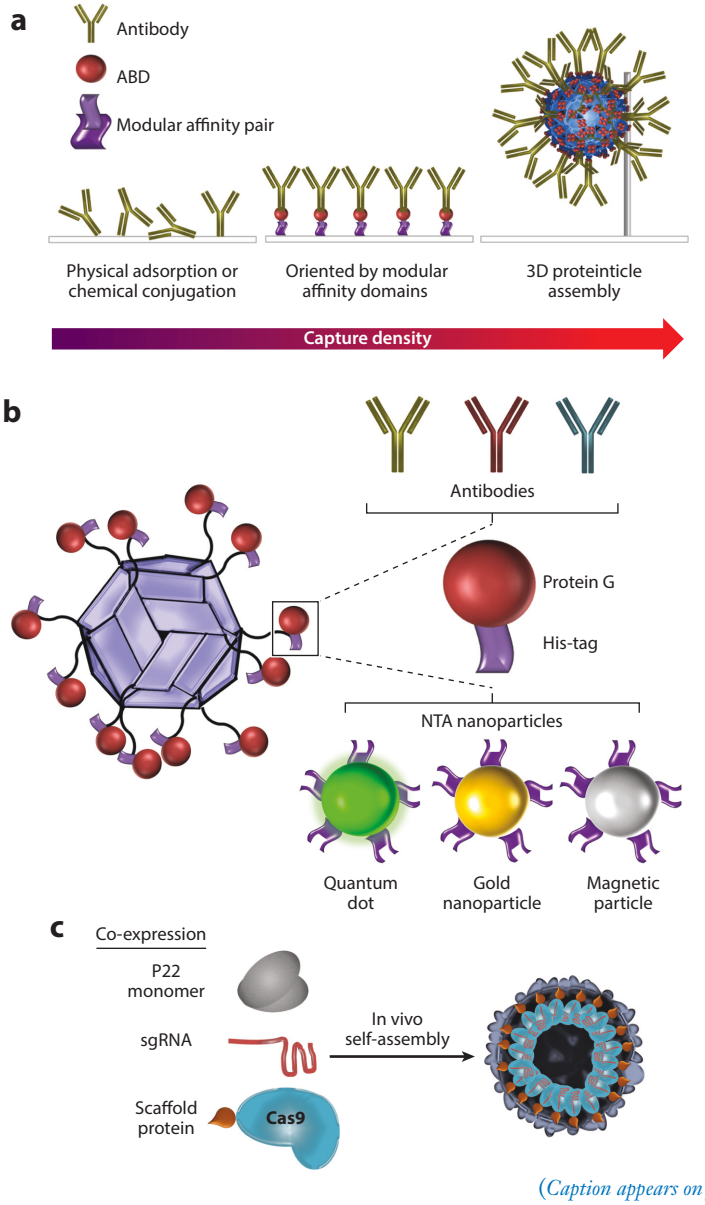

(*Caption appears on following page*)

Figure 4 (*Figure appears on preceding page*)

Applications of modular protein assembly in bioassays, bioimaging, and drug delivery and therapeutics. (*a*) Controlled immobilization of antibodies plays a critical role in bioassay performance. Orienting antibodies onto surfaces using a combination of ABDs and affinity domains increases antigen binding capacity over adsorption and random chemical conjugation. The available surface area for antibody capture can be further enhanced through 3D assembly of ABDs on proteinticles. (*b*) A modular bioimaging device was made by fusing human apoferritin monomers to protein G and a His-tag. These nanoscaffolds could be used to bind virtually any antibody of interest to any Ni-NTA-modified imaging agent of interest. Adapted with permission from Reference 67; copyright 2013 American Chemical Society. (*c*) Encapsulation of a wide variety of therapeutics holds promise in drug delivery applications. P22, for example, was used for the in vivo assembly of CRISPR-Cas9 proteins and gRNA into a single package via fusion of the Cas9 to its modular scaffolding domain. Abbreviations: ABD, antibody binding domain; CRISPR, clustered regularly interspaced short palindromic repeats; gRNA, guide RNA; NTA, nitrilotriacetic acid; sgRNA, single-guide RNA. Adapted with permission from Reference 129; copyright 2016 American Chemical Society.

vertices of the particles. The best-performing proteinticle was based on the HBV VLP because of its large size and high density of B domain. The HBV VLP contains 240 copies of its monomer subunit and was previously used to provide attomolar-level detection in an ELISA platform (61). The 3D platform was used to detect troponin I with a 100,000-fold higher sensitivity than previous ELISA platforms and could detect troponin I in acute myocardial infarction patients with 100% specificity, even at a 1,000× sera dilution.

For bioassay detection components, ABDs can serve as universal adaptors in linking a reporter to a sensing antibody. For example, Z-domain fused to glutathione-*S*-transferase coupled to three horseradish peroxidase (HRP) enzymes could bind to rabbit, rat, and mouse IgGs (66). Posttranslational conjugation is an attractive route for covalently linking reporters. Fluorescent dyes can be conjugated onto either the N or C terminus of an antibody using SrtA for a wide range of biosensing applications (111). Even enzymes can be ligated with antibodies to allow the use of common glucose meters for low-cost bioassays (112). Similarly, split-intein and native chemical ligation has allowed for the creation of sensing modules that employ small-molecule and protein reporters (113). The detection limit of bioassays, however, can be improved by providing higher signal amplification through multiple copies of a reporter.

One strategy for achieving signal amplification of a reporter is by linking tandem repeats of an ABD adapter to cluster antibodies at the antigen site (73). A poly protein G containing 8 repeating C2 domains (8pG) was used to decrease the detection limit by an order of magnitude in a direct ELISA and provided up to 50-fold higher signal in a sandwich ELISA. The 8pG also improved the detection limit of a Western blot by an order of magnitude and improved the fluorescence signal on labeled cells threefold without increasing the background. Signal amplification can also be achieved by linking the sensing domain to a protein nanoparticle containing multiple copies of the detection moiety (10, 26, 67). When the Z-domain was SrtA-ligated to an E2 nanocage displaying 22 copies of nanoluciferase, the sensitivity of immunodetection of thrombin was more than 20-fold higher than when using a fusion between the Z-domain and a single nanoluciferase (10). The structure of filamentous phage nanoparticles creates a unique platform for this type of signal amplification strategy (26). By fusing a tandem Z-domain to the P3 proteins on the end of the phage, the more than 4,000 P8 proteins that make up the body of the phage become available for decoration with a reporter moiety. Self-assembling amyloid nanowires can also provide high signal amplification (88). Biotinylated, BAP-fused Sup35 wire seeds were grown and then added to protein G–fused monomers and HRP–streptavidin for the creation of an amplified sensor that provided 2,000–4,000-fold higher signal than the conventional ELISA.

Bioimaging

Antibodies are frequently used as input components for imaging applications owing to their high binding and specificity, as well as their longevity in the blood for in vivo applications. Similar to the sensing applications, ABDs can also be used to link antibodies to imaging agents. A tandem Z-domain fused to a fluorogen-activating protein can be used to label surface receptors of live cells, fixed cells, and internal markers in permeabilized cells (114). Signal amplification can be obtained by linking the ABD to a nanoscaffold with multiple detection agents. Protein G fused to human apoferritin displaying quantum dots through Ni-NTA was able to provide a 27-fold increase in sensitivity in the detection of CLDN4 on pancreatic cancer cells compared with a fluorescently labeled antibody (67). Because the input and output domains are modularly incorporated, this imaging tool can be adapted toward virtually any target for immunofluorescence, electron microscopy, and MR imaging (**Figure 4*b***). Similarly, the Fc-III peptide fused to ferritin cages was used to image HER2 on SKBR3 breast cancer cells with trastuzumab and to image folate on KB cells with rabbit antifolate antibodies (77). Although ABDs based off protein A or G can be used as a secondary mimic, the limitation in using these in imaging applications is the inability to multiplex different fluorophores with species-specific antibodies.

Covalent, site-specific labeling of antibodies can be done with photoactivable ADBs or posttranslational ligation strategies. HER-2-expressing SKOV-3 cells were imaged via confocal microscopy using photoactivable, FAM-labeled Z-domain conjugated to trastuzumab (81). A combination of intein chemistry and photoactivable Z-domain was used to label rituximab with a 10–amino acid peptide containing a fluorophore and bio-orthogonal azide group. Click chemistry was then used to covalently link superparamagnetic iron oxide nanoparticles for MR imaging (80). Posttranslational strategies are particularly useful for labeling small antibody fragments used for imaging applications that require high binding and penetration of targeted tissue but rapid clearance from the rest of the body. SrtA-mediated ligation of the bifunctional chelator MeCoSar to the scFv anti-LIBS (ligand-induced binding site) has allowed the delivery and coordination of the $^{64}Cu^{2+}$ radioactive isotope for positron emission tomography imaging of mouse artery thrombosis by binding to activated platelets in the area of interest (115).

Nanocages are of particular interest for bioimaging, as they can be loaded with molecules such as fluorophores and contrast agents for MR imaging applications. A sHsp nanocage was engineered to encapsulate fluorescent dyes and was exteriorly decorated with a small peptide, LyP-1, to target tumor-associated macrophages (116). This dually modified sHsp was used as an imaging agent for diagnosis of atherosclerosis. sHsp nanocages have also been explored for MR imaging. Specifically, gadolinium was anchored to the interior of sHsp by genetically engineering a metal-binding peptide into the cage subunits, and the encapsulated contrast agent showed increased relaxivity rates (117). Ferritin has been used frequently in the encapsulation of contrast agents because of its inherent assembly/disassembly properties and small pore size. Gadolinium was encapsulated by first dissociating the ferritin nanocage at pH 2 then neutralizing the pH back to 7 for reassembly (118). Similarly, Cy5.5-labeled ferritin genetically modified to incorporate the RGD peptide was used encapsulate radioactive copper (119). This loaded ferritin nanocage was applied toward in vivo imaging.

Drug Delivery and Therapeutics

Many drug therapies under investigation require high dosages that cause considerable discomfort to patients owing to their lack of targeting mechanisms. Because nanoscaffolds can be modified with external input domains to target tissues of interest, as well as their ability to load output

therapeutic cargos such as chemotherapeutics, siRNA, RNA used for genome editing and cellular programming, and proteins (12, 120), they harbor the potential to enhance therapeutic efficacy (32).

One of the most popular applications of engineered nanoscaffolds is for targeted chemotherapy drug delivery. Ferritin has often been shown to encapsulate a variety of small molecules, such as methylene blue, which was shown to have cytotoxic effects on MCF-7 human breast cancer cells upon light-induced release (121), as well as the anticancer drugs cisplatin, carboplatin (122), 5-fluorouracil, daunomycin, and doxorubicin (123, 124). sHsp has also been genetically modified to encapsulate doxorubicin. Flenniken et al. (125) described a robust method for delivering this anticancer drug with a pH-dependent release mechanism. Another group expanded upon the sHsp-encapsulated doxorubicin method by genetically engineering the cages to express a hepatoma-binding peptide on the exterior of the capsid for targeted delivery of the anticancer drug to human hepatocellular carcinoma cells (126). The newly engineered S19 nanocages could also be loaded with the hydrophobic anticancer drug doxorubicin through hydrophobic interactions and showed controlled release of the drug at pH 5 both in vitro and in vivo (55). These findings suggest that the S19 nanocage can be applied to the encapsulation of other hydrophobic drugs and pH-controlled release.

Nanoscaffolds have also been explored as nanocarriers for therapeutic nucleic acids. The MS2 capsids were genetically engineered into MS2-coat-retrovirus chimeras to package biologically active RNAs for delivery to various cell types, including human CD34 and induced pluripotent stem cells. This group applied the MS2-encapsulated RNA toward transient gene expression, showing successful production of the Cre-recombinase for widespread editing at the ROSA26 locus. These findings suggest that this technology can be applied to other delivery applications, such as cellular programming and genome editing (127). Ferritins have been shown to encapsulate siRNA for gene silencing with incorporation of cationic peptides (21). The HBV capsid protein has also been genetically engineered to express the capsid protein fused to a p19 RNA-binding protein as well as an integrin-binding peptide (RGD). This chimeric protein self-assembles into a nanocage that has dual affinity for siRNA on the interior of the cage and integrin receptors on the exterior. This dual decorated quality of the HBV chimera allows for targeted delivery of siRNA (128). S-19 nanocages protect DNA in the interior for gene therapy applications (55).

The P22 capsid was engineered to encapsulate a Cas9 protein as well as a single-guide RNA that remains functional for sequence-specific cleavage of targeted DNA (**Figure 4*c***). This nuclease active Cas9 cargo platform could circumvent delivery issues prevalent with Cas9 therapeutics (129). Although the Cas9-sgRNA (single-guide RNA) complexes are protected from degradation after encapsulation, this strategy cannot release the complex once internalized. An improved strategy has been reported in which P22 is engineered to encapsulate bioactive peptide therapeutics that serves as a tunable nanocarrier capable of crossing the blood–brain barrier. A ring-opening metathesis polymerization (ROMP) reaction was employed to trigger the P22 nanocage to disassemble under physiological conditions, exposing the bioactive peptides for targeting. Specifically, a substrate for ROMP (norbornene) was conjugated to the exterior of the P22 nanocage, and when triggered with Grubbs II Catalyst, the cage disassembled, leading to the release of encapsulated molecules (130). This strategy may be combined with Cas9 delivery to enable the intracellular release.

Antibodies are frequently used as input domains in therapeutic targeting. A simple means of deploying cytotoxic outputs, such as chemotherapies or bacterial and plant toxins, to a specific tissue is by tethering them directly to an antibody. Because chemical methods can result in an inhomogeneous pool of antibody–chemical conjugates, site-specific conjugation schemes are important for therapeutic efficacy. Using split inteins, Frutos et al. (131) linked anti-HER2 antibodies to

the cytotoxic drug Cys-Auristain F, thus creating enzymatically linked antibody–drug conjugates. Anti-HER1 antibodies have also been conjugated to the plant toxin gelonin (132) by using split inteins, indicating that both protein and small-molecule drugs can be combined with antibodies for therapeutic goals. Compared with split inteins, SrtA technology requires minimal genetic modification to the antibody. SrtA generated equivalents to brentuximab-vedotin (α-CD30) and trastuzumab-maytasine antibody–drug conjugates, which demonstrated similar or better antitumor activity than their chemically conjugated counterparts (133). SrtA-mediated ligation of the α-HER2 antibody to the plant toxin gelonin increased the antitumor properties of gelonin by 1,000-fold (134). Photoactivable ABDs can be used for Fc-specific conjugation without any genetic modification requirements to the antibody. Photoactivable Fc-III peptide was used to label trastuzumab with a bacterial toxin (82) and small-molecule drugs (135) for delivery into cancer cells.

NUCLEIC ACID–BASED SCAFFOLDS FOR PROTEIN ASSEMBLY

Although protein-based scaffolds provide a highly modular platform for multi-functionalization, they generally lack the ability for highly dynamic assembly for conditional release and adaptive cell targeting. The ability to easily predict and manipulate the base-pairing property of nucleic acids, along with the ease of synthesis, has allowed researchers to create various DNA- or RNA-based nanoscaffolds and dynamically programmable nanostructures (136, 137). These nanoscaffolds could serve as sensing, delivery, and therapeutics platforms, especially when coupled with functional proteins (138, 139).

Compared with RNA, DNA has many properties that make it a good platform for protein scaffolding. It is stabler and can be programmed into homogeneous nanostructures with sizes ranging from 50 to 400 nm, which is optimal for drug delivery with enhanced permeability and retention effect in tumor regions (140). DNA can serve as a loading pad for cargos with multiple functions (e.g., therapeutic payloads and targeting ligands). DNA origami can also be programmed into 3D containers with encapsulation and stimuli-triggered release functions as smart delivery vehicles (141). Different chemotherapeutic drugs (141), nanoparticles (142), therapeutic expression vectors (143), and aptamers were either individually assembled or coassembled on DNA origami for tumor targeting. These technologies showed robust antitumor effects without apparent systemic toxicity. DNA origami is unique in its programmable nanostructures and stimuli-responsive functions. Li et al. (144) developed a DNA nanorobot system to deliver active thrombin, which regulates platelet aggregation, to tumor sites to induce obstructive thrombosis. Thrombin was loaded into a tubular DNA nanorobot with targeting aptamers at both ends (**Figure 5*b***). The nanocarriers, after delivery, opened in response to the presence of nucleolin to expose the encapsulated thrombin. By using these responsive DNA nanorobots, they delivered therapeutic thrombin in vivo to tumor-associated blood vessels to elicit highly efficient blockage of tumor blood supply and inhibit tumor growth (144). This nanorobot strategy also holds promise for conditional Cas9 delivery, a benefit difficult to achieve using VLP encapsulation. Although DNA stability was previously tested both in cell lysates and with live cells (145), there is still a need to make DNA nanorobots more robust in the complex human environment. There is also a need to expand design responsiveness so the delivery vehicle can respond to a broader spectrum of stimuli.

Another example of responsive nucleic acid structures are molecular beacons (MBs). MBs are single-stranded stem-loop DNA probes widely used for sensitive and specific detection of nucleic acids (146). The stem-loop structure comes with a fluorophore-labeled 5′ end and a quencher-labeled 3′ end that in close proximity result in minimal fluorescence. A significant increase in fluorescence is detected when the stem-loop structure opens spontaneously in the presence of a

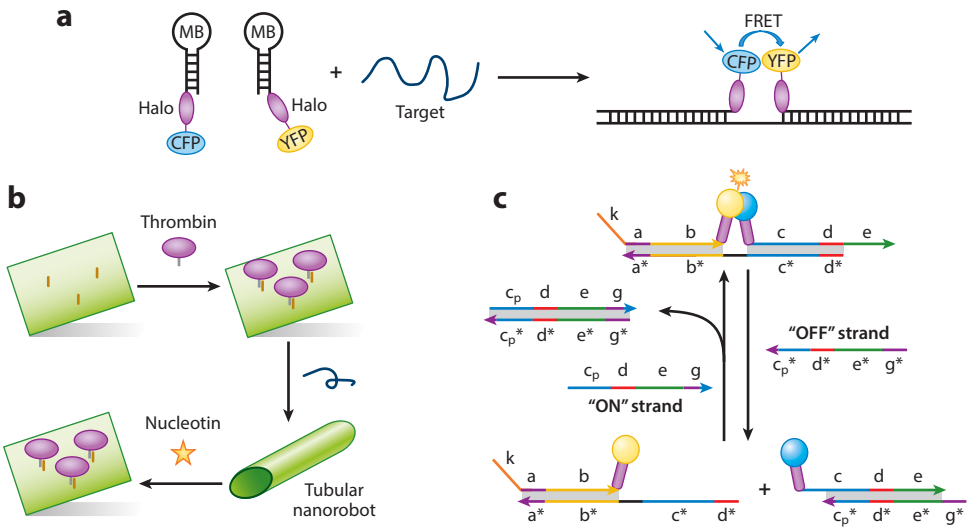

Figure 5

Nucleotide-based protein organization for diagnosis, delivery, and therapy. (*a*) Fluorescent protein–decorated MB for sensing applications. (*b*) A tubular nanorobot for thrombin encapsulation and stimuli (nucleotin)-triggered thrombin exposure. Binding of nucleotin to the aptamer domain releases thrombin from the nanorobot to the tumor site. (*c*) Programmed control of protein assembly for precise activation of anticancer therapy. Toehold-mediated strand displacement is used to trigger the assembly of two split yeast cytosine deaminase fragments, which catalyze deamination of a nontoxic prodrug into a chemotherapeutic agent, only in the presence of two different miRNA inputs. Abbreviations: CFP, cyan fluorescent protein; FRET, fluorescence resonance energy transfer; MB, molecular beacon; YFP, yellow fluorescent protein.

single-stranded nucleotide sequence complementary to the loop region. However, the complexity and high cost associated with the dual labeling are potential issues for more widespread usage (147). To alleviate these problems, attempts have been made to replace the fluorophore/quencher pair with fluorescence proteins (148) (**Figure 5*a***). By using the DNA-binding functionality of zinc finger proteins, a new class of fluorescence protein–MBs was created and exhibited the same high specificity and selectivity for detection. A second version using the HaloTag protein to provide covalent conjugation to a chlorohexane-modified DNA oligo was designed to further improve stability and effectiveness (148). For the detection of nucleic acid analytes, DNA and RNA dynamic scaffolds can be employed to convert inputs to readable signals. The SpyTag/SpyCatcher system has also been used to covalently link a TEV protease to single-stranded DNA sequences to create a protease-dependent sensor for sensing specific single-stranded DNA and RNA strands (149).

Toehold-mediated strand displacement, which involves revealing a new sequence in response to the binding of an initiator strand, is another powerful way to design dynamic DNA scaffolds for therapeutic applications (18). Multiple displacement reactions can be linked into a cascade in which the newly revealed output sequence of one reaction can initiate another displacement step elsewhere (150). By taking advantage of this cascading capability, multiple miRNAs were explored to achieve programmable control of prodrug activation (**Figure 5*c***). This was accomplished by dynamically modulating the reconstitution of two split yeast cytosine deaminase fragments, which catalyze deamination of a nontoxic prodrug into a chemotherapeutic agent (18). This programming system can sense the environment, process the information via a predefined signal-processing algorithm, and actuate based on the results of the computation (151). Another benefit is the ability to provide signal amplification through regeneration of the input strand for

ultrasensitive therapeutic activation. A similar strategy was reported to provide spatiotemporal control over gene silencing, in which a small conditional RNA was conditionally activated into a functional siRNA by multiple strand-displacement operations (152). Even DNA-gated lock-and-key devices have been designed for controlled release applications (141). These examples highlight the modularity of the strand-displacement approach to elicit a wide range of conditional protein phenotypes that are suitable for diagnosis, delivery, and therapy applications.

CONCLUSIONS AND FUTURE OUTLOOKS

Herein, we have demonstrated how the modular assembly of proteins into well-defined nanostructures has provided unique functionalities for a variety of biomedical applications. Self-assembling protein cages provide robust and uniform scaffolds, whereas nucleic acids provide a dynamic and programmable platform that is responsive to endogenous stimuli. Assembly strategies based on biological building blocks and enzymatically derived conjugations offer site-specific control over the presentation of input and output domains and were shown to outperform traditional chemical strategies in a variety of contexts. The nanostructures enhance the capabilities of the input and output domains through signal amplification, avidity of binding domains, and high therapeutic payloads. When these devices are assembled in a modular format, they can easily be readapted for different targets and applications.

Natural nanoscaffolds, such as viral-like particles and nanocages, have inherent properties that make them ideal platforms for biosensing and delivery, and the flexibility of these platforms in tolerating modifications has been widely explored. Although research in the development of these particles for in vitro sensing and imaging devices is quite mature, there are challenges in creating the ideal delivery vehicle for in vivo applications. For scaffolds of nonhuman origin, safety and immunogenicity concerns remain. Furthermore, the combination of efficient cargo encapsulation with an endogenous stimuli-responsive release mechanism remains a work in progress. De novo design of synthetic protein–based cages offers potential in addressing these design concerns. Synthetic nanocages could be constructed using humanized protein building blocks, and further inspiration can be taken from nature into the design of loading and release strategies. For example, the P22 phage, which has one of the most efficient cargo loading strategies, contains a separate scaffolding domain that docks into the interior face of the capsid. Although current icosahedral, synthetic cages contain two separate blocks for controlled assembly upon mixing, a third block could be incorporated to specifically load internal cargo prior to assembly. For disassembly, the CCMV capsid provides a unique pH-responsive mechanism. Design of a physiologically relevant pH switch into the scaffold platform could be an area of exploration for these synthetic cages.

Whereas proteins create robust static nanoscaffolds, nucleic acids offer a more responsive platform for drug delivery. Nucleic acid scaffolds have been programmed to respond to endogenous nucleic acids, proteins, and small molecules, which are physiologically relevant stimuli that could be used as triggers for cargo release. Further, nucleic acids can process multiple inputs with Boolean logic. Combining the dynamic scaffolding of nucleic acids with functional protein output domains has already shown promise in sensing and smart therapeutics. This concept could be expanded through integration into synthetic protein scaffolds for stimuli-responsive cage disassembly and cargo release. Disassembly programmed from multi-input architecture could increase target specificity and allow the design of smart nanomaterials for personalized medicine.

DISCLOSURE STATEMENT

The authors are not aware of any affiliations, memberships, funding, or financial holdings that might be perceived as affecting the objectivity of this review.

ACKNOWLEDGMENTS

This review was supported by grants from the National Science Foundation (CBET1803008, CBET1604925, and DMR1609621).

LITERATURE CITED

1. Zhang Y, Chan HF, Leong KW. 2013. Advanced materials and processing for drug delivery: the past and the future. *Adv. Drug Deliv. Rev.* 65:104–20
2. Papapostolou D, Howorka S. 2009. Engineering and exploiting protein assemblies in synthetic biology. *Mol. BioSyst.* 5:723–32
3. Qi Y, Ge H. 2006. Modularity and dynamics of cellular networks. *PLOS Comput. Biol.* 2:e174
4. Sowmya G, Breen EJ, Ranganathan S. 2015. Linking structural features of protein complexes and biological function. *Protein Sci.* 24:1486–94
5. Mallagaray A, Creutznacher R, Dülfer J, Mayer PHO, Grimm LL, et al. 2019. A post-translational modification of human Norovirus capsid protein attenuates glycan binding. *Nat. Commun.* 10:1320
6. Roos WH, Ivanovska IL, Evilevitch A, Wuite GJ. 2007. Viral capsids: mechanical characteristics, genome packaging and delivery mechanisms. *Cell. Mol. Life Sci.* 64:1484–97
7. Chen Q, Sun Q, Molino NM, Wang S-W, Boder ET, Chen W. 2015. Sortase A-mediated multifunctionalization of protein nanoparticles. *Chem. Commun.* 51:12107–10
8. Raeeszadeh-Sarmazdeh M, Hartzell E, Price JV, Chen W. 2016. Protein nanoparticles as multifunctional biocatalysts and health assessment sensors. *Curr. Opin. Chem. Eng.* 13:109–18
9. Jordan PC, Patterson DP, Saboda KN, Edwards EJ, Miettinen HM, et al. 2015. Self-assembling biomolecular catalysts for hydrogen production. *Nat. Chem.* 8:179–85
10. Sun Q, Chen Q, Blackstock D, Chen W. 2015. Post-translational modification of bionanoparticles as a modular platform for biosensor assembly. *ACS Nano* 9:8554–61
11. Lieser RM, Chen W, Sullivan MO. 2019. Controlled epidermal growth factor receptor ligand display on cancer suicide enzymes via unnatural amino acid engineering for enhanced intracellular delivery in breast cancer cells. *Bioconjugate Chem.* 30:432–42
12. Rohovie M, Nagasawa M, Swartz J. 2017. Virus-like particles: next-generation nanoparticles for targeted therapeutic delivery. *Bioeng. Transl. Med.* 2:43–57
13. Veronese FM, Mero A. 2008. The impact of PEGylation on biological therapies. *BioDrugs* 22:315–29
14. Mao HY, Hart SA, Schink A, Pollok BA. 2004. Sortase-mediated protein ligation: a new method for protein engineering. *J. Am. Chem. Soc.* 126:2670–71
15. Swartz AR, Chen W. 2018. SpyTag/SpyCatcher functionalization of E2 nanocages with stimuli-responsive Z-ELP affinity domains for tunable monoclonal antibody binding and precipitation properties. *Bioconjugate Chem.* 29:3113–21
16. Cristie-David AS, Sciore A, Badieyan S, Escheweiler JD, Koldewey P, et al. 2017. Evaluation of *de novo*-designed coiled coils as off-the-shelf components for protein assembly. *Mol. Syst. Des. Eng.* 2:140–48
17. Patterson DP, Prevelige PE, Douglas T. 2012. Nanoreactors by programmed enzyme encapsulation inside the capsid of the bacteriophage P22. *ACS Nano* 6:5000–9
18. Chen RP, Blackstock D, Sun Q, Chen W. 2018. Dynamic protein assembly by programmable DNA strand displacement. *Nat. Chem.* 10:474–81
19. Heddle J, Chakraborti S, Iwasaki K. 2017. Natural and artificial protein cages: design, structure and therapeutic applications. *Curr. Opin. Struct. Biol.* 43:148–55
20. Aniagyei S, DuFort C, Kao C, Dragnea B. 2008. Self-assembly approaches to nanomaterial encapsulation in viral protein cages. *J. Mater. Chem.* 18:3763–74
21. Lee E, Lee S, Kang Y, Ryu J, Kwon K, et al. 2015. Engineered proteinticles for targeted delivery of siRNA to cancer cells. *Adv. Funct. Mater.* 25:1279–86
22. Wen A, Steinmetz N. 2016. Design of virus-based nanomaterials for medicine, biotechnology, and energy. *Chem. Soc. Rev.* 45:4074–126
23. Brown S, Fiedler J, Finn M. 2009. Assembly of hybrid bacteriophage Qβ virus-like particles. *Biochemistry* 48:11155–57

24. Bundy B, Swartz J. 2011. Efficient disulfide bond formation in virus-like particles. *J. Biotechnol.* 154:230–39
25. Patterson DP, Schwarz B, Waters RS, Gedeon T, Douglas T. 2014. Encapsulation of an enzyme cascade within the bacteriophage P22 virus-like particle. *ACS Chem. Biol.* 9:359–65
26. Brasino M, Lee JH, Cha JN. 2015. Creating highly amplified enzyme-linked immunosorbent assay signals from genetically engineered bacteriophage. *Anal. Biochem.* 470:7–13
27. Glasgow J, Tullman-Ercek D. 2014. Production and applications of engineered viral capsids. *Appl. Microbiol. Biotechnol.* 98:5847–58
28. Walker A, Skamel C, Nassal M. 2011. SplitCore: an exceptionally versatile viral nanoparticle for native whole protein display regardless of 3D structure. *Sci. Rep.* 1:5
29. Schoonen L, Eising S, van Eldijk MB, Bresseleers J, van der Pijl M, et al. 2018. Modular, bioorthogonal strategy for the controlled loading of cargo into a protein nanocage. *Bioconjugate Chem.* 29:1186–93
30. Lee EJ, Lee E, Kim HJ, Lee JH, Ahn KY, et al. 2014. Self-assembled proteinticle nanostructures for 3-dimensional display of antibodies. *Nanoscale* 6:14919–25
31. Harrison P, Arosio P. 1996. Ferritins: molecular properties, iron storage function and cellular regulation. *Biochim. Biophys. Acta* 1275:161–203
32. Lee E, Lee N, Kim I. 2016. Bioengineered protein-based nanocage for drug delivery. *Adv. Drug Deliv. Rev.* 106:157–71
33. Jakob U, Gaestel M, Engel K, Buchner J. 1993. Small heat-shock proteins are molecular chaperones. *J. Biol. Chem.* 268:1517–20
34. Kim K, Kim R, Kim S. 1998. Crystal structure of a small heat-shock protein. *Nature* 394:595–99
35. Murata M, Narahara S, Kawano T, Hamano N, Piao J, et al. 2015. Design and function of engineered protein nanocages as a drug delivery system for targeting pancreatic cancer cells via neuropilin-1. *Mol. Pharm.* 12:1422–30
36. Swartz AR, Sun Q, Chen W. 2017. Ligand-induced cross-linking of Z-elastin-like polypeptide-functionalized E2 protein nanoparticles for enhanced affinity precipitation of antibodies. *Biomacromolecules* 18:1654–59
37. Bhaskar S, Lim S. 2017. Engineering protein nanocages as carriers for biomedical applications. *NPG Asia Mater.* 9:e371
38. Padilla JE, Colovos C, Yeates TO. 2001. Nanohedra: using symmetry to design self assembling protein cages, layers, crystals, and filaments. *PNAS* 98:2217–21
39. Sinclair JC, Davies KM, Venien-Bryan C, Noble MEM. 2011. Generation of protein lattices by fusing proteins with matching rotational symmetry. *Nat. Nano* 6:558–62
40. King NP, Bale JB, Sheffler W, McNamara DE, Gonen S, et al. 2014. Accurate design of co-assembling multi-component protein nanomaterials. *Nature* 510:103–8
41. Sugimoto K, Kanamaru S, Iwasaki K, Arisaka F, Yamashita I. 2006. Construction of a ball-and-spike protein supramolecule. *Angew. Chem.* 45:2725–28
42. Lai Y-T, Reading E, Hura GL, Tsai K-L, Laganowsky A, et al. 2014. Structure of a designed protein cage that self-assembles into a highly porous cube. *Nat. Chem.* 6:1065–71
43. Gradisar H, Bozic S, Doles T, Vengust D, Hafner-Bratkovic I, et al. 2013. Design of a single-chain polypeptide tetrahedron assembled from coiled-coil segments. *Nat. Chem. Biol.* 9:362–66
44. Sciore A, Su M, Koldewey P, Eschweiler JD, Diffley KA, et al. 2016. Flexible, symmetry-directed approach to assembling protein cages. *PNAS* 113:8681–86
45. King NP, Sheffler W, Sawaya MR, Vollmar BS, Sumida JP, et al. 2012. Computational design of self-assembling protein nanomaterials with atomic level accuracy. *Science* 336:1171–74
46. Bale JB, Gonen S, Liu Y, Sheffler W, Ellis D, et al. 2016. Accurate design of megadalton-scale two-component icosahedral protein complexes. *Science* 353:389–94
47. Kostal J, Mulchandani A, Chen W. 2001. Tunable biopolymers for heavy metal removal. *Macromolecules* 34:2257–61
48. MacKay JA, Chen M, McDaniel JR, Liu W, Simnick AJ, Chilkoti A. 2009. Self-assembling chimeric polypeptide-doxorubicin conjugate nanoparticles that abolish tumours after a single injection. *Nat. Mater.* 8:993–99

49. Costa SA, Mozhdehi D, Dzuricky MJ, Isaacs FJ, Brustad EM, Chilkoti A. 2019. Active targeting of cancer cells by nanobody decorated polypeptide micelle with bio-orthogonally conjugated drug. *Nano Lett*. 19:247–54
50. Fletcher J, Harniman R, Barnes F, Boyle A, Collins A, et al. 2013. Self-assembling cages from coiled-coil peptide modules. *Science* 340:595–99
51. Zaccai NR, Chi B, Thomson AR, Boyle AL, Bartlett GJ, et al. 2011. A *de novo* peptide hexamer with a mutable channel. *Nat. Chem. Biol.* 7:935–41
52. Ljubetič A, Lapenta F, Gradišar H, Drobnak I, Aupič J, et al. 2017. Design of coiled-coil protein-origami cages that self-assemble *in vitro* and *in vivo*. *Nat. Biotechnol.* 35:1094–101
53. Park WM, Champion JA. 2014. Thermally triggered self-assembly of folded proteins into vesicles. *J. Am. Chem. Soc.* 136:17906–9
54. Ding D, Guerette P, Fu J, Zhang L, Irvine S, Miserez A. 2015. From soft self-healing gels to stiff films in suckerin-based materials through modulation of crosslink density and β-sheet content. *Adv. Mater.* 27:3953–61
55. Ping Y, Ding D, Ramos R, Mohanram H, Deepankumar K, et al. 2017. Supramolecular β-sheets stabilized protein nanocarriers for drug delivery and gene transfection. *ACS Nano* 11:4528–41
56. Uchida M, Flenniken ML, Allen M, Willits DA, Crowley BE, et al. 2006. Targeting of cancer cells with ferrimagnetic ferritin cage nanoparticles. *J. Am. Chem. Soc.* 128:16626–33
57. Choi K-M, Kim K, Kwon IC, Kim I-S, Ahn HJ. 2013. Systemic delivery of siRNA by chimeric capsid protein: tumor targeting and RNAi activity *in vivo*. *Mol. Pharm.* 10:18–25
58. Yoo L, Park J-S, Kwon KC, Kim S-E, Jin X, et al. 2012. Fluorescent viral nanoparticles with stable *in vitro* and *in vivo* activity. *Biomaterials* 33:6194–200
59. van Vught R, Pieters RJ, Breukink E. 2014. Site-specific functionalization of proteins and their applications to therapeutic antibodies. *Comput. Struct. Biotechnol. J.* 9:e201402001
60. De Las Rivas J, Fontanillo C. 2010. Protein-protein interactions essentials: key concepts to building and analyzing interactome networks. *PLOS Comput. Biol.* 6:e1000807
61. Park JS, Cho MK, Lee EJ, Ahn KY, Lee KE, et al. 2009. A highly sensitive and selective diagnostic assay based on virus nanoparticles. *Nat. Nanotechnol.* 4:259–64
62. Jung YW, Lee JM, Kim JW, Yoon JW, Cho HM, Chung BH. 2009. Photoactivable antibody binding protein: site-selective and covalent coupling of antibody. *Anal. Chem.* 81:936–42
63. Jung YW, Kang HJ, Lee JM, Jung SO, Yun WS, et al. 2008. Controlled antibody immobilization onto immunoanalytical platforms by synthetic peptide. *Anal. Biochem.* 374:99–105
64. Richman DD, Cleveland PH, Oxman MN, Johnson KM. 1982. The binding of staphylococcal protein-A by the sera of different animal species. *J. Immunol.* 128:2300–5
65. Guss B, Eliasson M, Olsson A, Uhlen M, Frej AK, et al. 1986. Structure of the IGG-binding regions of streptococcal protein-G. *EMBO J.* 5:1567–75
66. Min J, Song EK, Kim H, Kim KT, Park TJ, Kang S. 2016. A recombinant secondary antibody mimic as a target-specific signal amplifier and an antibody immobilizer in immunoassays. *Sci. Rep.* 6:10
67. Hwang MP, Lee JW, Lee KE, Lee KH. 2013. Think modular: a simple apoferritin-based platform for the multifaceted detection of pancreatic cancer. *ACS Nano* 7:8167–74
68. Bjorck L, Kronvall G. 1984. Purification and some properties of streptococcal protein-G, protein-A novel IGG-binding reagent. *J. Immunol.* 133:969–74
69. Nilsson B, Moks T, Jansson B, Abrahmsen L, Elmblad A, et al. 1987. A synthetic IGG-binding domain based on staphylococcal protein-A. *Protein Eng.* 1:107–13
70. Graille M, Stura EA, Corper AL, Sutton BJ, Taussig MJ, et al. 2000. Crystal structure of a *Staphylococcus aureus* protein A domain complexed with the Fab fragment of a human IgM antibody: structural basis for recognition of B-cell receptors and superantigen activity. *PNAS* 97:5399–404
71. Ljungquist C, Jansson B, Moks T, Uhlen M. 1989. Thiol-directed immobilization of recombinant IGG-binding receptors. *Eur. J. Biochem.* 186:557–61
72. Sauer-Eriksson AE, Kleywegt GJ, Uhlén M, Jones TA. 1995. Crystal-structure of the C2 fragment of streptococcal protein-G in complex with the FC domain of human-IGG. *Structure* 3:265–78

73. Chen YJ, Chen M, Cheng TL, Roffler SR, Lin SY, et al. 2019. Simply mixing poly protein G with detection antibodies enhances the detection limit and sensitivity of immunoassays. *Anal. Chem.* 91:8310–17
74. Feng B, Huang SR, Ge F, Luo YP, Jia DY, Dai YZ. 2011. 3D antibody immobilization on a planar matrix surface. *Biosens. Bioelectron.* 28:91–96
75. Choe W, Durgannavar TA, Chung SJ. 2016. Fc-binding ligands of immunoglobulin G: an overview of high affinity proteins and peptides. *Materials* 9:994
76. DeLano WL, Ultsch MH, de Vos AM, Wells JA. 2000. Convergent solutions to binding at a protein-protein interface. *Science* 287:1279–83
77. Kang HJ, Kang YJ, Lee YM, Shin HH, Chung SJ, Kang S. 2012. Developing an antibody-binding protein cage as a molecular recognition drug modular nanoplatform. *Biomaterials* 33:5423–30
78. Yu FF, Alesand V, Nygren P-Å. 2018. Site-specific photoconjugation of beta-lactamase fragments to monoclonal antibodies enables sensitive analyte detection via split-enzyme complementation. *Biotechnol. J.* 13:e1700688
79. Westerlund K, Vorobyeva A, Mitran B, Orlova A, Tolmachev V, et al. 2019. Site-specific conjugation of recognition tags to trastuzumab for peptide nucleic acid-mediated radionuclide HER2 pretargeting. *Biomaterials* 203:73–85
80. Hui JZ, Al Zaki A, Cheng ZL, Popik V, Zhang HT, et al. 2014. Facile method for the site-specific, covalent attachment of full-length IgG onto nanoparticles. *Small* 10:3354–63
81. Perols A, Famme MA, Karlström AE. 2015. Site-specific antibody labeling by covalent photoconjugation of Z domains functionalized for alkyne-azide cycloaddition reactions. *ChemBioChem* 16:2522–29
82. Park J, Lee Y, Ko BJ, Yoo TH. 2018. Peptide-directed photo-cross-linking for site-specific conjugation of IgG. *Bioconjugate Chem.* 29:3240–44
83. Sano T, Cantor CR. 2000. Streptavidin-containing chimeric proteins: design and production. *Methods Enzymol.* 326:305–11
84. Cui XP, Vasylieva N, Shen D, Barnych B, Yang J, et al. 2018. Biotinylated single-chain variable fragment-based enzyme-linked immunosorbent assay for glycocholic acid. *Analyst* 143:2057–65
85. Beckett D, Kovaleva E, Schatz PJ. 1999. A minimal peptide substrate in biotin holoenzyme synthetase-catalyzed biotinylation. *Protein Sci.* 8:921–29
86. Valadon P, Darsow B, Buss TN, Czarny M, Griffin NM, et al. 2010. Designed auto-assembly of nanostreptabodies for rapid tissue-specific targeting *in vivo*. *J. Biol. Chem.* 285:713–22
87. Zhu M, Gong X, Hu YH, Ou WJ, Wan YK. 2014. Streptavidin-biotin-based directional double Nanobody sandwich ELISA for clinical rapid and sensitive detection of influenza H5N1. *J. Transl. Med.* 12:352
88. Men D, Zhang ZP, Guo YC, Zhu DH, Bi LJ, et al. 2010. An auto-biotinylated bifunctional protein nanowire for ultra-sensitive molecular biosensing. *Biosens. Bioelectron.* 26:1137–41
89. Thrane S, Janitzek CM, Agerbaek MØ, Ditlev SB, Resende M, et al. 2015. A novel virus-like particle based vaccine platform displaying the placental malaria antigen VAR2CSA. *PLOS ONE* 10:e0143071
90. Tienken L, Drude N, Schau I, Winz OH, Temme A, et al. 2018. Evaluation of a pretargeting strategy for molecular imaging of the prostate stem cell antigen with a single chain antibody. *Sci. Rep.* 8:3755
91. Block H, Maertens B, Spriestersbach A, Brinker N, Kubicek J, et al. 2009. Immobilized-metal affinity chromatography (IMAC): a review. In *Guide to Protein Purification*, ed. RR Burgess, MP Deutscher, 463:439–73. San Diego, CA: Elsevier Acad. 2nd ed.
92. Hochuli E, Bannwarth W, Dobeli H, Gentz R, Stüber D. 1988. Genetic approach to facilitate purification of recombinant proteins with a novel metal chelate adsorbent. *Nat. Biotechnol.* 6:1321–25
93. Le DHT, Commandeur U, Steinmetz NF. 2019. Presentation and delivery of tumor necrosis factor-related apoptosis-inducing ligand via elongated plant viral nanoparticle enhances antitumor efficacy. *ACS Nano* 13:2501–10
94. Goldsmith LE, Pupols M, Kickhoefer VA, Rome LH, Monbouquette HG. 2009. Utilization of a protein "shuttle" to load vault nanocapsules with gold probes and proteins. *ACS Nano* 3:3175–83

95. Matsuura K, Nakamura T, Watanabe K, Noguchi T, Minamihata K, et al. 2016. Self-assembly of Ni-NTA-modified β-annulus peptides into artificial viral capsids and encapsulation of His-tagged proteins. *Org. Biomol. Chem.* 14:7869–74
96. Antos JM, Truttmann MC, Ploegh HL. 2016. Recent advances in sortase-catalyzed ligation methodology. *Curr. Opin. Struct. Biol.* 38:111–18
97. Dorr BM, Ham HO, An C, Chaikof EL, Liu DR. 2014. Reprogramming the specificity of sortase enzymes. *PNAS* 111:13343–48
98. Hess GT, Cragnolini JJ, Popp MW, Allen MA, Dougan SK, et al. 2012. M13 bacteriophage display framework that allows sortase-mediated modification of surface-accessible phage proteins. *Bioconjugate Chem.* 23:1478–87
99. Shah NH, Muir TW. 2014. Inteins: nature's gift to protein chemists. *Chem. Sci.* 5:446–61
100. Paulus H. 2000. Protein splicing and related forms of protein autoprocessing. *Annu. Rev. Biochem.* 69:447–96
101. Lockless SW, Muir TW. 2009. Traceless protein splicing utilizing evolved split inteins. *PNAS* 106:10999–1004
102. Siu K-H, Chen W. 2017. Control of the yeast mating pathway by reconstitution of functional α-factor using split intein-catalyzed reactions. *ACS Synth. Biol.* 6:1453–60
103. Zakeri B, Fierer JO, Celik E, Chittock EC, Schwarz-Linek U, et al. 2012. Peptide tag forming a rapid covalent bond to a protein, through engineering a bacterial adhesin. *PNAS* 109:E690–97
104. Fierer JO, Veggiani G, Howarth M. 2014. SpyLigase peptide-peptide ligation polymerizes affibodies to enhance magnetic cancer cell capture. *PNAS* 111:E1176–81
105. Veggiani G, Nakamura T, Brenner MD, Gayet RV, Yan J, et al. 2016. Programmable polyproteams built using twin peptide superglues. *PNAS* 113:1202–7
106. Tan LL, Hoon SS, Wong FT. 2016. Kinetic controlled tag-catcher interactions for directed covalent protein assembly. *PLOS ONE* 11:e0165074
107. Brune KD, Buldun CM, Li YY, Taylor IJ, Brod F, et al. 2017. Dual plug-and-display synthetic assembly using orthogonal reactive proteins for twin antigen immunization. *Bioconjugate Chem.* 28:1544–51
108. Nguyen DL, Kim H, Kim D, Lee JO, Gye MC, Kim YP. 2018. Detection of matrix metalloproteinase activity by bioluminescence via intein-mediated biotinylation of luciferase. *Sensors* 18:875
109. Madej MP, Coia G, Williams CC, Caine JM, Pearce LA, et al. 2012. Engineering of an anti-epidermal growth factor receptor antibody to single chain format and labeling by sortase A-mediated protein ligation. *Biotechnol. Bioeng.* 109:1461–70
110. Anderson GP, Liu JL, Shriver-Lake LC, Zabetakis D, Sugiharto VA, et al. 2019. Oriented immobilization of single-domain antibodies using SpyTag/SpyCatcher yields improved limits of detection. *Anal. Chem.* 91:9424–29
111. Chen L, Cohen J, Song X, Zhao A, Ye Z, et al. 2016. Improved variants of SrtA for site-specific conjugation on antibodies and proteins with high efficiency. *Sci. Rep.* 6:31899
112. Ismail NF, Lim TS. 2016. Site-specific scFv labelling with invertase via Sortase A mechanism as a platform for antibody-antigen detection using the personal glucose meter. *Sci. Rep.* 6:19338
113. Jeon H, Lee E, Kim D, Lee M, Ryu J, et al. 2018. Cell-based biosensors based on intein-mediated protein engineering for detection of biologically active signaling molecules. *Anal. Chem.* 90:9779–86
114. Gallo E, Vasilev KV, Jarvik J. 2014. Fluorogen-activating-proteins as universal affinity biosensors for immunodetection. *Biotechnol. Bioeng.* 111:475–84
115. Paterson BM, Alt K, Jeffery CM, Price RI, Jagdale S, et al. 2014. Enzyme-mediated site-specific bioconjugation of metal complexes to proteins: sortase-mediated coupling of copper-64 to a single-chain antibody. *Angew. Chem.* 53:6115–19
116. Uchida M, Kosuge H, Terashima M, Willits DA, Liepold LO, et al. 2011. Protein cage nanoparticles bearing the LyP-1 peptide for enhanced imaging of macrophage-rich vascular lesions. *ACS Nano* 5:2493–502
117. Liepold L, Abedin M, Buckhouse E, Frank J, Young M, Douglas T. 2009. Supramolecular protein cage composite MR contrast agents with extremely efficient relaxivity properties. *Nano Lett.* 9:4520–26

118. Aime S, Frullano L, Crich S. 2002. Compartmentalization of a gadolinium complex in the apoferritin cavity: a route to obtain high relaxivity contrast agents for magnetic resonance imaging. *Angew. Chem.* 41:1017–19
119. Lin X, Xie J, Niu G, Zhang F, Gao H, et al. 2011. Chimeric ferritin nanocages for multiple function loading and multimodal imaging. *Nano Lett.* 11:814–19
120. Ma Y, Nolte R, Cornelissen J. 2012. Virus-based nanocarriers for drug delivery. *Adv. Drug Deliv. Rev.* 64:811–25
121. Yan F, Zhang Y, Yuan H, Gregas M, Vo-Dinh T. 2008. Apoferritin protein cages: a novel drug nanocarrier for photodynamic therapy. *Chem. Commun.* 38:4579–81
122. Yang Z, Wang X, Diao H, Zhang J, Li H, et al. 2007. Encapsulation of platinum anticancer drugs by apoferritin. *Chem. Commun.* 33:3453–55
123. Liang M, Fan K, Zhou M, Duan D, Zheng J, et al. 2014. H-ferritin-nanocaged doxorubicin nanoparticles specifically target and kill tumors with a single-dose injection. *PNAS* 111:14900–5
124. Bellini M, Mazzucchelli S, Galbiati E, Sommaruga S, Fiandra L, et al. 2014. Protein nanocages for self-triggered nuclear delivery of DNA-targeted chemotherapeutics in cancer cells. *J. Control. Release* 196:184–96
125. Flenniken M, Liepold L, Crowley B, Willits D, Young M, Douglas T. 2005. Selective attachment and release of a chemotherapeutic agent from the interior of a protein cage architecture. *Chem. Commun.* 28:447–49
126. Toita R, Murata M, Abe K, Narahara S, Piao J, et al. 2013. A nanocarrier based on a genetically engineered protein cage to deliver doxorubicin to human hepatocellular carcinoma cells. *Chem. Commun.* 49:7442–44
127. Prel A, Caval V, Gayon R, Ravassard P, Duthoit C, et al. 2015. Highly efficient *in vitro* and *in vivo* delivery of functional RNAs using new versatile MS2-chimeric retrovirus-like particles. *Mol. Therapy Methods Clin. Dev.* 2:15039
128. Choi K-M, Choi SH, Jeon H, Kim IS, Ahn HJ. 2011. Chimeric capsid protein as a nanocarrier for siRNA delivery: stability and cellular uptake of encapsulated siRNA. *ACS Nano* 5:8690–99
129. Qazi S, Miettinen H, Wilkinson R, McCoy K, Douglas T, Wiedenheft B. 2016. Programmed self-assembly of an active P22-Cas9 nanocarrier system. *Mol. Pharm.* 13:1191–96
130. Kelly P, Anand P, Uvaydov A, Chakravartula S, Sherpa C, et al. 2015. Developing a dissociative nanocontainer for peptide drug delivery. *Int. J. Environ. Res. Public Health* 12:12543–55
131. Frutos S, Hernández JL, Otero A, Calvis C, Adan J, et al. 2018. Site-specific antibody drug conjugates using streamlined expressed protein ligation. *Bioconjugate Chem.* 29:3503–8
132. Pirzer T, Becher KS, Rieker M, Meckel T, Mootz HD, Kolmar H. 2018. Generation of potent anti-HER1/2 immunotoxins by protein ligation using split inteins. *ACS Chem. Biol.* 13:2058–66
133. Beerli RR, Hell T, Merkel AS, Grawunder U. 2015. Sortase enzyme-mediated generation of site-specifically conjugated antibody drug conjugates with high *in vitro* and *in vivo* potency. *PLOS ONE* 10:e0131177
134. Kornberger P, Skerra A. 2014. Sortase-catalyzed in vitro functionalization of a HER2-specific recombinant Fab for tumor targeting of the plant cytotoxin gelonin. *mAbs* 6:354–66
135. Vance N, Zacharias N, Ultsch M, Li GM, Fourie A, et al. 2019. Development, optimization, and structural characterization of an efficient peptide-based photoaffinity cross-linking reaction for generation of homogeneous conjugates from wild-type antibodies. *Bioconjugate Chem.* 30:148–60
136. Pinheiro A, Han D, Shih W, Yan H. 2011. Challenges and opportunities for structural DNA nanotechnology. *Nat. Nanotechnol.* 6:763–72
137. Hong F, Zhang F, Liu Y, Yan H. 2017. DNA origami: scaffolds for creating higher order structures. *Chem. Rev.* 117:12584–640
138. Fu J, Yang Y, Johnson-Buck A, Liu M, Liu Y, et al. 2014. Multi-enzyme complexes on DNA scaffolds capable of substrate channelling with an artificial swinging arm. *Nat. Nanotechnol.* 9:531–36
139. Berckman E, Chen W. 2019. Exploiting dCas9 fusion proteins for dynamic assembly of synthetic metabolons. *Chem. Commun.* 55:8219–22
140. Chauhan V, Jain R. 2013. Strategies for advancing cancer nanomedicine. *Nat. Mater.* 12:958–62

141. Douglas S, Bachelet I, Church G. 2012. A logic-gated nanorobot for targeted transport of molecular payloads. *Science* 335:831–34
142. Du Y, Jiang Q, Beziere N, Song L, Zhang Q, et al. 2016. DNA-nanostructure-gold-nanorod hybrids for enhanced in vivo optoacoustic imaging and photothermal therapy. *Adv. Mater.* 28:10000–7
143. Liu J, Song L, Liu S, Jiang Q, Liu Q, et al. 2018. A DNA-based nanocarrier for efficient gene delivery and combined cancer therapy. *Nano Lett.* 18:3328–34
144. Li S, Jiang Q, Liu S, Zhang Y, Tian Y, et al. 2018. A DNA nanorobot functions as a cancer therapeutic in response to a molecular trigger *in vivo*. *Nat. Biotechnol.* 36:258–64
145. Shen X, Jiang Q, Wang J, Dai L, Zou G, et al. 2012. Visualization of the intracellular location and stability of DNA origami with a label-free fluorescent probe. *Chem. Commun.* 48:11301–3
146. Monroy-Contreras R, Vaca L. 2011. Molecular beacons: powerful tools for imaging RNA in living cells. *J. Nucleic Acids* 2011:741723
147. Blackstock D, Sun Q, Chen W. 2015. Fluorescent protein-based molecular beacons by zinc finger protein-guided assembly. *Biotechnol. Bioeng.* 112:236–41
148. Blackstock D, Chen W. 2014. Halo-tag mediated self-labeling of fluorescent proteins to molecular beacons for nucleic acid detection. *Chem. Commun.* 50:13735–38
149. Park HJ, Yoo TH. 2018. Nucleic acid detection by a target-assisted proximity proteolysis reaction. *ACS Sens.* 3:2066–70
150. Zhang D, Seelig G. 2011. Dynamic DNA nanotechnology using strand-displacement reactions. *Nat. Chem.* 3:103–13
151. Han D, Zhu Z, Wu C, Peng L, Zhou L, et al. 2012. A logical molecular circuit for programmable and autonomous regulation of protein activity using DNA aptamer-protein interactions. *J. Am. Chem. Soc.* 134:20797–804
152. Hochrein LM, Schwarzkopf M, Shahgholi M, Yin P, Pierce NA. 2013. Conditional dicer substrate formation via shape and sequence transduction with small conditional RNAs. *J. Am. Chem. Soc.* 135:17322–30

Annual Review of Chemical and Biomolecular Engineering

Volume 11, 2020

Contents

Errata

An online log of corrections to *Annual Review of Chemical and Biomolecular Engineering* articles may be found at http://www.annualreviews.org/errata/chembioeng